Available online at www.sciencedirect.com
ScienceDirect
Trans. Nonferrous Met. Soc. China 28(2018) 574−584
Transactions of Nonferrous Metals Society of China
www.tnmsc.cn

Phase equilibria in Ti−Ni−Pt ternary system

Yue ZHONG, Yue SUN, Hua-shan LIU, Ge-mei CAI, Zhan-peng JIN

School of Materials Science and Engineering, Central South University, Changsha 410083, China

Received 13 October 2016; accepted 20 February 2017

Abstract: Phase equilibria in Ti−Ni−Pt ternary system have been experimentally determined through diffusion triple technique combined with alloy samples approach. Assisted with electron probe microanalysis (EPMA) and X-ray diffraction (XRD) techniques, isothermal sections at 1073 and 1173 K of this system were constructed and existence of ternary phase $Ti_2(Ni,Pt)_3$ was confirmed. In addition, binary compounds Ti_3Pt_5 and $TiPt_{3-}$ were found to be stable at 1073 and 1173 K, and remarkable ternary solubility in some binary compounds was detected, e.g., solubility of Pt in TiNi can be up to about 36% (molar fraction) at 1073 K and 40% (molar fraction) at 1173 K. Furthermore, a ternary invariant transition reaction $TiNi_3+Ti_3Pt_5\rightarrow Ti_2(Ni,Pt)_3+TiPt_{3+}$ at a temperature between 1073 and 1173 K was deduced.

Key words: Ti−Ni−Pt ternary system; phase equilibrium; diffusion triple; solubility

1 Introduction

Titanium−nickel shape memory alloys (SMAs) are widely used in medical and industrial fields because of their superior shape memory effect and superelasticity [1−3]. However, high-temperature applications of TiNi alloys are limited because their martensite transformation temperatures (M_s) are commonly lower than 373 K [4]. Variety of studies have been performed to raise M_s of TiNi with addition of Pt [5,6], focusing on introducing precipitates which are helpful to minimize residual strain and obtain better dimensional stability [7] and oxidative stability [8]. Several types of precipitations can be introduced in several TiNiPt alloys [9], e.g. a fine coherent *P*-phase precipitate after aging at 873 K for 100 h [10] or $Ti_2(Ni,Pt)_3$ phase precipitates after aging at 873 K [11,12]. In order to provide reference in developing high-temperature shape memory alloys (HTSMAs) and well comprehending precipitations in TiNiPt alloys, knowledge concerning phase relationships of Ti−Ni−Pt system is of fundamental importance.

So far, boundary binary phase equilibria in Ti−Ni−Pt system have been widely studied. The Ni−Pt phase diagram appears simple, showing mainly the isomorphous feature between liquid and disordered FCC-solid solution at high temperature besides the order-disorder transitions at low temperature. NASH and SINGLETON [13] performed a thermodynamic assessment of liquid and FCC phase. Later, LU et al [14] re-assessed the Ni−Pt system by considering ordered phases Ni_3Pt-*L*12, NiPt-*L*10 and $NiPt_3$-*L*12 at lower temperature.

The Ti−Ni system was firstly calculated by KAUFMAN and NESOR [15]. The most recent critical assessment of the system has been carried out by MURRAY [16] who considered literature data up to 1985. Later, this system has been thoroughly investigated by several authors [17−22]. Recently, POVODEN-KARADENIZ et al [23] re-optimized this system by taking account of new thermodynamic data for *D*024-ordered $TiNi_3$ phase along with two metastable phases Ti_3Ni_4 and Ti_2Ni_3. It is accepted that the Ti−Ni system contains four stable intermetallics, i.e. $TiNi_3$, Ti_2Ni, TiNi(h) and TiNi(r).

Dissimilar to the Ti−Ni system, only a few equilibrium studies about the Ti−Pt binary system were reported. Phase diagram of Ti−Pt system was firstly constructed by NISHIMURA and HIRAMATSU [24]. MURRAY [25] evaluated and assessed this system in detail. Later, BIGGS et al [26] detected a phase Ti_4Pt_3 in compositional range of 30%−60%Pt (molar fraction).

Foundation item: Project (2016YFB0701404) supported by the National Key Research and Development Program of China; Project (51171210) supported by the National Natural Science Foundation of China

Corresponding author: Hua-shan LIU; Tel: +86-731-88876735; Fax: +86-731-88876692; E-mail: hsliu@csu.edu.cn

DOI: 10.1016/S1003-6326(18)64690-4

Recently, LI et al [27] have re-assessed the Ti−Pt system thermodynamically, considering homogeneity ranges of Ti_3Pt, TiPt(h), TiPt(r) and $TiPt_{3+}$ phases, while neglecting Ti_3Pt_5 and $TiPt_{3-}$ phase. The Ti_4Pt_3 and $TiPt_8$ phases were treated as stoichiometric compounds, for having an unnoticeable and uncertain solubility range. It is worth noting that $TiPt_{3-}$ and $TiPt_{3+}$ are different phases, respectively denoting the Pt-lean and the Pt-rich $TiPt_3$ phase.

Phase relations in the Ti−Ni−Pt ternary system are far from being accomplished. Only the ternary phase $Ti_2(Ni,Pt)_3$ reported by YANG et al [12] is available. It is obvious that the phase diagram is the map of material design. In order to assist the design and fabrication of Ti−Ni based alloys, extensive investigation of phase equilibria in the Ti−Ni−Pt ternary system is necessary. Crystal structure data for solid phases in Ti−Ni−Pt system are summarized in Table 1. This work aims at measuring phase equilibria in the Ti−Ni−Pt ternary system at 1073 and 1173 K.

2 Experimental

Pure titanium (99.999% Ti), nickel (99.99% Ni), and platinum (99.99% Pt) were used as starting materials for diffusion triple and alloys. To fabricate diffusion couples, titanium block and nickel block were machined into proper shapes (cuboid with size of 3 mm × 5 mm × 10 mm). The platinum wire with diameter of 0.5 mm was nipped between titanium and nickel blocks, and then was heated to and kept at 1173 K for 10 h for diffusion-bonding in a chamber filled with Ar of 10^{-2} Pa. Subsequently, the so-obtained triples were sealed in evacuated quartz capsules and then annealed at 1073 K for 1000 h and 1173 K for 500 h. After annealing, diffusion triples were taken out of the diffusion furnace and quenched into water.

In order to confirm the relations determined with diffusion triple, a set of button alloys in different compositions were prepared by arc-melting on a water-cooled copper plate under purified argon atmosphere with titanium as getter material placed in the arc chamber. To ensure a good homogenization, all samples were turned over before each melting and re-melted at least three times. The mass losses of the so-obtained as-cast button shaped alloys did not exceed 1%. Subsequently, majority of samples were sealed in evacuated quartz capsules and then heat-treated at 1073 K for 2000 h and at 1173 K for 1000 h. After annealing, those annealed diffusion triples and button-alloys were taken out of the diffusion furnace and quenched into water. And they were ground on abrasive paper, polished with diamond paste and cleaned with alcohol in a standard method.

Constituent phases of samples were investigated by electron probe microanalysis (EPMA) (JXA−8800R, JEOL, Japan) equipped with OXFORD INCA 500 wavelength dispersive X-ray spectrometer (WDS). The

Table 1 Crystallographic data of solid phases in Ti−Ni−Pt system from references

System	Phase	Prototype	Pearson's symbol	Lattice parameter			Ref.
				a/nm	*b*/nm	*c*/nm	
Ti	HCP-A3, *α*(Ti)	Mg	*hp*2	0.2950	0.2950	0.4681	[28]
	BCC-A2, *β*(Ti)	W	*cI*2	0.3307	0.3307	0.3307	[28]
Ni	FCC-A1, (Ni)	Cu	*cF*4	0.35236	0.35236	0.35236	[29]
Pt	FCC-A1, (Pt)	Cu	*cF*4	0.39234	0.39234	0.39234	[30]
Ti−Ni	Ti_2Ni	Ti_2Ni	*cF*96	1.13193	1.13193	1.13193	[31]
	TiNi(h) (>353 K)	ClCs	*cP*2	0.3007	0.3007	0.3007	[31]
	TiNi(r) (<353 K)	TiNi	*mP*4	0.2898	0.4108	0.4646	[31]
	$TiNi_3$	$TiNi_3$	*hP*16	0.51088	0.51088	0.83187	[29]
Ti−Pt	Ti_3Pt	Cr_3Si	*cP*8	0.50327	0.50327	0.50327	[32]
	Ti_4Pt_3	–	–	–	–	–	[26]
	TiPt(h) (>1307 K)	CsCl	*cP*2	0.3129	0.3129	0.3129	[33]
	TiPt(r) (<1313 K)	AuCd	*oP*4	0.459	0.276	0.482	[34]
	Ti_3Pt_5	$GaZn_2Au_5$	*oI*32	1.0953	0.5441	0.8169	[35]
	$TiPt_{3-}$	$TiNi_3$	*hP*16	0.552	0.552	0.9019	[36]
	$TiPt_{3+}$	$AuCu_3$	*cP*4	0.3923	0.3923	0.3923	[37]
	$TiPt_8$	$TiPt_8$	*tI*18	0.8312	0.8312	0.3897	[38]
Ti−Ni−Pt	$Ti_2(Ni,Pt)_3$	Ti_2Pd_3	*oC*20	1.359	0.457	0.444	[39]

acceleration voltage is 15 kV and the wavelengths used for Ti, Ni and Pt are 2.7485 Å ($K_{\alpha 1}$), 1.6579 Å ($K_{\alpha 1}$) and 6.047 Å ($M_{\alpha 1}$), respectively. The corresponding spectrometer crystals used for Ti, Ni and Pt are PETJ, LIF and PETH, respectively. Standard deviations of the measured concentration are ±0.6% (molar fraction). The total mass fraction of elements Ti, Ni, and Pt in each phase is in the range of 97%−103%. The compositions reported in this work were the average values of three measurements. X-ray diffraction (XRD) was also performed to the annealed alloys using a Cu K_{α} radiation on a Rigaku D-max/2550VB+ X-ray diffractometer at 40 kV and 250 mA in continuous mode with a step size of 0.02° at a speed of 8 (°)/min.

3 Results and discussion

3.1 Phase equilibria at 1073 K

Phase relations covering the entire composition range of the Ti−Ni−Pt ternary system at 1073 K were studied by combining diffusion triple and alloy sampling methods. Figure 1 presents the BSE images of Ti−Ni−Pt diffusion triple annealed at 1073 K for 1000 h. During the long-term annealing, most of the equilibrium phases were formed and can be easily identified in the diffusion triple. The tri-junction area in the sample reflects phase equilibrium information in the ternary system. It is apparent that three layers of phases were formed between the end-members Ti and Ni. With EPMA, these layers were detected to be Ti_2Ni, TiNi and $TiNi_3$, respectively. Similarly, seven layers of intermetallics, i.e., Ti_3Pt, Ti_4Pt_3, TiPt, Ti_3Pt_5, $TiPt_{3-}$, $TiPt_{3+}$ and $TiPt_8$, were formed between Ti and Pt. Obviously, most of the compounds observed here are in good agreement with those in Ti−Ni and Ti−Pt binary systems, except for the controversial phases Ti_3Pt_5 and $TiPt_{3-}$ which were considered to be unstable at 1073 K [25]. Furthermore, a ternary phase was detected, of which the composition can be expressed as $Ti_{40}(Ni,Pt)_{60}$, similar to that of the ternary phase $Ti_2(Ni,Pt)_3$ reported by YANG et al [12], so it was regarded as $Ti_2(Ni,Pt)_3$.

Phases and their locations in diffusion triple annealed at 1073 K are schematically illustrated in Fig. 2. Each curve represents an interface between two adjacent phases, and each tri-junction point stands for a three-phase equilibrium. Based on the assumption of local equilibrium, the tie-line information was obtained from composition profiles of the EPMA scans across phase interfaces. The detailed method to extract phase equilibrium through diffusion triple is referred to JIN [40,41]. Phase-relations obtained from diffusion triple at 1073 K are summarized in Table 2.

A number of 18 alloys were prepared to confirm or supplement phase relations of the Ti−Ni−Pt system at 1073 K. Figure 3 shows constituent phases in alloy A3 and alloy A7. As seen from Fig. 3(a) , alloy A3 locates in the three-phase area of Ti_3Pt + TiNi + Ti_2Ni. This is confirmed by X-ray diffraction (Fig. 3(b)). Also,

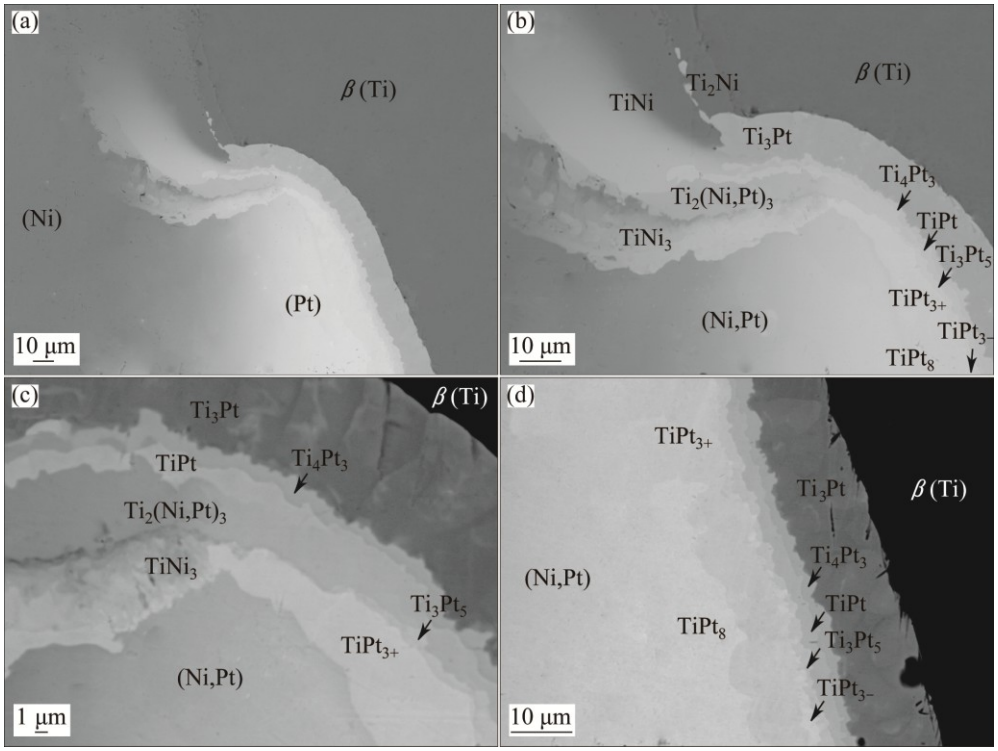

Fig. 1 Backscattered electron (BSE) images of Ti−Ni−Pt diffusion triple annealed at 1073 K for 1000 h: (a) Panorama; (b−d) Magnified parts

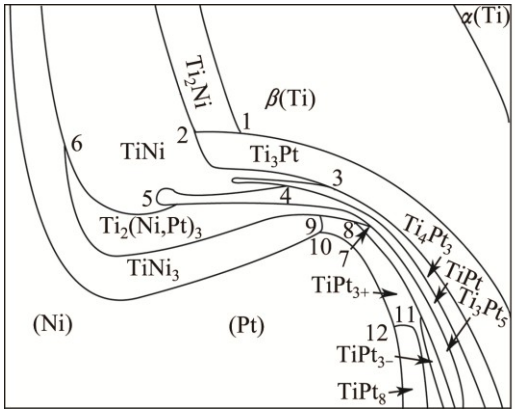

Ternary equilibria:
1: β(Ti)+Ti_2Ni+Ti_3Pt
2: Ti_2Ni+TiNi+Ti_3Pt
3: TiNi+Ti_3Pt+Ti_4Pt_3
4: TiNi+Ti_4Pt_3+TiPt
5: TiNi+TiPt+$Ti_2(Ni,Pt)_3$
6: TiNi+$TiNi_3$+$Ti_2(Ni,Pt)_3$
7: $Ti_2(Ni,Pt)_3$+Ti_3Pt_5+TiPt
8: $Ti_2(Ni,Pt)_3$+Ti_3Pt_5+$TiPt_{3+}$
9: $TiNi_3$+$Ti_2(Ni,Pt)_3$+$TiPt_{3+}$
10: $TiNi_3$+$TiPt_{3+}$+(Ni,Pt)
11: Ti_3Pt_5+$TiPt_{3-}$+$TiPt_{3+}$
12: (Ni,Pt)+$TiPt_{3+}$+$TiPt_8$

Fig. 2 Schematic diagram of phase distribution in diffusion triple at 1073 K (numbered tri-junction points (1−12) represent ternary equilibria existing in Ti−Ni−Pt system)

Table 2 Tie-lines determined through Ti−Ni−Pt diffusion triple treated at 1073 K

Tie-line	Phase composition (molar fraction)/%					
Phase 1/Phase 2	Phase 1			Phase 2		
	Ti	Ni	Pt	Ti	Ni	Pt
α(Ti)/β(Ti)	95.8	4.1	0.1	98.2	1.7	0.1
	97.1	1.9	1.0	98.5	0.7	0.8
β(Ti)/Ti_2Ni	92.0	6.2	1.8	68.2	31.1	0.7
	91.5	6.5	2.0	67.6	31.6	0.8
β(Ti)/Ti_3Pt	91.7	6.5	1.8	75.7	1.8	22.5
	91.8	5.4	2.8	74.8	0.4	24.8
Ti_2Ni/Ti_3Pt	67.9	31.2	0.9	74.8	1.4	23.8
	67.5	31.3	1.2	75.4	2.1	22.5
Ti_2Ni/TiNi	67.3	31.6	1.1	50.8	48.8	0.4
	67.4	31.3	1.3	50.3	49.2	0.5
TiNi/Ti_3Pt	51.1	24.2	24.7	74.2	0.9	24.9
	50.7	29.3	20.0	75.0	0.8	24.2
	51.5	29.7	18.8	74.5	0.8	24.7
	50.9	47.3	1.8	74.4	1.4	24.2
	51.1	48.0	0.9	75.1	1.7	23.2
TiNi/Ti_4Pt_3	51.9	16.1	32.0	58.5	4.0	37.5
	51.3	23.3	25.4	58.6	4.5	36.9
	50.5	21.2	28.3	59.1	3.0	37.9
Ti_3Pt/Ti_4Pt_3	74.6	0.2	25.2	58.9	2.3	38.8
	72.7	0.5	26.8	58.0	2.1	39.9
TiNi/TiPt	50.4	14.2	35.4	49.8	4.3	45.9
	50.9	14.5	34.6	49.8	4.3	45.9
Ti_4Pt_3/TiPt	58.4	2.5	39.1	51.4	3.0	45.6
	58.3	0.7	41.0	49.5	0.6	49.9
TiNi/$Ti_2(Ni,Pt)_3$	48.6	40.8	10.6	40.4	42.9	16.7
	49.6	22.9	27.5	39.9	39.7	20.4
	49.2	34.5	16.3	40.4	40.7	18.9
	49.8	17.2	33.0	40.2	34.5	25.3
TiPt/$Ti_2(Ni,Pt)_3$	49.1	2.9	48.0	40.4	17.3	42.3
	49.2	5.5	45.3	40.5	28.1	31.4
	48.9	1.9	49.2	40.3	13.1	46.6
	48.2	1.4	50.4	40.0	10.0	50.0
TiNi/$TiNi_3$	47.9	50.0	2.1	25.3	74.7	0.0

Tie-line	Phase composition (molar fraction)/%					
Phase 1/Phase 2	Phase 1			Phase 2		
	Ti	Ni	Pt	Ti	Ni	Pt
$TiNi_3$/$Ti_2(Ni,Pt)_3$	25.9	66.8	7.3	40.1	42.5	17.4
	25.0	62.4	12.6	39.3	40.1	20.6
	25.1	49.2	25.7	39.6	34.7	25.7
	25.5	59.4	15.1	39.3	35.3	25.4
	25.9	36.8	37.3	40.1	28.6	31.3
	25.3	27.2	47.5	39.9	26.9	33.2
	24.7	22.2	53.1	40.0	15.1	44.9
TiPt/Ti_3Pt_5	48.8	0.9	50.3	38.3	0.5	61.2
	50.2	0.5	49.3	38.5	4.1	57.4
Ti_3Pt_5/$Ti_2(Ni,Pt)_3$	37.2	5.8	57.0	40.1	10.0	49.9
$TiPt_{3+}$/$Ti_2(Ni,Pt)_3$	25.5	9.2	65.3	40.0	12.9	47.1
	25.4	8.1	66.5	40.0	12.4	47.6
Ti_3Pt_5/$TiPt_{3-}$	37.7	0.5	61.8	26.8	0.2	73.0
$TiPt_{3-}$/$TiPt_{3+}$	26.6	0.2	73.2	24.3	0.6	75.1
Ti_3Pt_5/$TiPt_{3+}$	37.1	5.3	57.6	25.1	5.4	69.5
	38.1	0.5	61.4	24.9	3.8	71.3
	38.2	0.2	61.6	25.2	1.8	73.0
$TiNi_3$/$TiPt_{3+}$	23.9	21.7	54.4	22.8	13.5	63.7
	24.7	22.2	53.1	23.6	12.4	64.0
$TiNi_3$/(Ni,Pt)	23.4	69.6	7.0	5.8	93.2	1.0
	23.7	64.2	12.1	4.8	93.1	2.1
	22.4	48.3	29.3	3.7	86.6	9.7
	22.6	38.6	38.8	2.6	83.4	14.0
	20.4	32.4	47.2	2.1	72.1	25.8
	20.9	27.3	51.8	1.3	56.6	42.1
	22.0	24.7	53.3	0.5	50.4	49.1
$TiPt_{3+}$/(Ni,Pt)	19.6	14.2	66.2	0.5	48.4	51.1
	19.8	9.5	70.7	0.3	35.2	64.5
	20.3	7.5	72.2	0.3	22.2	77.5
$TiPt_{3+}$/$TiPt_8$	19.8	4.5	75.7	11.3	2.8	85.9
	20.7	3.4	75.9	10.6	1.5	87.9
	20.5	2.1	77.4	11.6	0.5	87.9
$TiPt_8$/(Ni,Pt)	10.1	2.4	87.5	0.2	14.9	84.9
	9.7	2.1	88.2	1.7	5.7	92.6
	10.5	0.4	89.1	1.3	3.9	94.8
	10.7	0.0	89.3	0.9	1.9	97.2

microstructure of alloy A7 is shown in Fig. 3(c). With EPMA−WDS, it is known that alloy A7 consists of β(Ti), Ti_2Ni and Ti_3Pt, in accordance with XRD results (Fig. 3(d)).

Back-scattered electron (BSE) micrograph of alloy A8 is presented in Fig. 4(a), where two phases can be observed, which are the gray $TiNi_3$ and the white $Ti_2(Ni,Pt)_3$, in consistence with the XRD patterns shown in Fig. 4(b). $Ti_2(Ni,Pt)_3$ was also detected in alloys A6, A9, A12 and A13.

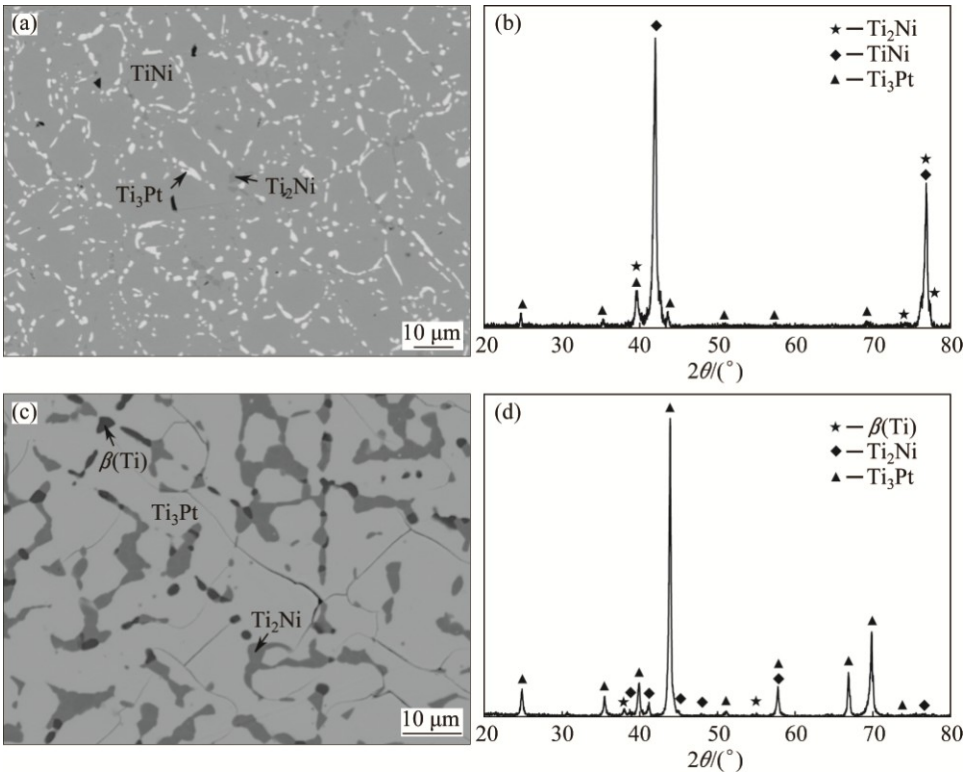

Fig. 3 BSE images and XRD patterns of alloys A3 (a, b) and A7 (c, d) annealed at 1073 K for 2000 h

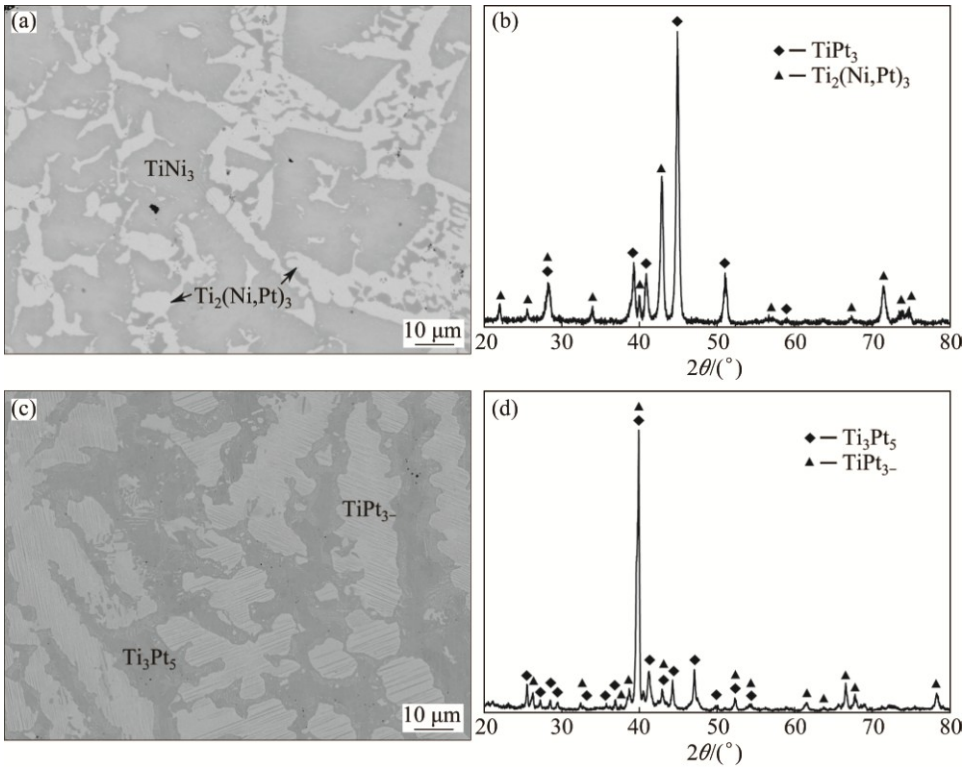

Fig. 4 BSE images and XRD patterns of alloys A8 (a, b) and A18 (c, d) annealed at 1073 K for 2000 h

Especially, in order to judge whether Ti_3Pt_5 and $TiPt_{3-}$ are stable or not at 1073 K, an additional alloy A18 with the nominal composition of Ti32Pt68 was further prepared. Figures 4(c) and (d) demonstrate that A18 consists of two phases, Ti_3Pt_5 and $TiPt_{3-}$. That is to say, these two phases can be stable at 1073 K.

Detected phases and their corresponding compositions in different annealed alloys are listed in Table 3. It can be seen later, phase relations obtained through alloy sampling were well consistent with those from diffusion triple.

Based on experimental results obtained in this measurement and relevant binary systems in literatures, the isothermal section of Ti−Ni−Pt ternary system at 1073 K is established, as shown in Fig. 5, where 12 three-phase regions were determined. It is worth noting

Table 3 Phases and their compositions in Ti−Ni−Pt alloys annealed at 1073 K

Alloy	Composition (molar fraction)/%	Phase equilibrium			Phase composition (molar fraction)/%								
		Phase 1	Phase 2	Phase 3	Phase 1			Phase 2			Phase 3		
					Ti	Ni	Pt	Ti	Ni	Pt	Ti	Ni	Pt
A1	Ti10Ni65Pt25	$TiNi_3$	(Ni,Pt)	−	20.3	42.2	37.5	2.6	84.1	13.3	−	−	−
A2	Ti30Ni65Pt5	TiNi	$TiNi_3$	−	25.8	70.8	3.4	48.2	43.4	8.4	−	−	−
A3	Ti55Ni40Pt5	Ti_2Ni	TiNi	Ti_3Pt	67.5	31.5	1.0	52.0	47.0	1.0	73.5	3.9	22.6
A4	Ti70Ni25Pt5	Ti_2Ni	Ti_3Pt	−	67.2	30.8	2.0	73.9	3.8	22.3	−	−	−
A5	Ti90Ni5Pt5	β(Ti)	Ti_3Pt	−	92.9	4.5	2.6	76.7	1.1	22.2	−	−	−
A6	Ti40Ni40Pt20	$Ti_2(Ni,Pt)_3$	−	−	39.9	39.9	20.2	−	−	−	−	−	−
A7	Ti75Ni5Pt20	β(Ti)	Ti_2Ni	Ti_3Pt	92.4	5.4	2.2	68.4	30.6	1.0	75.8	0.7	23.5
A8	Ti30Ni45Pt25	$TiNi_3$	$Ti_2(Ni,Pt)_3$	−	25.1	49.7	25.2	39.6	35.2	25.2	−	−	−
A9	Ti25Ni70Pt5	$TiNi_3$	$Ti_2(Ni,Pt)_3$	−	25.1	69.3	5.6	39.6	45.2	15.2	−	−	−
A10	Ti50Ni25Pt25	TiNi	Ti_3Pt	−	49.2	25.9	24.9	74.7	1.0	24.3	−	−	−
A11	Ti70Ni5Pt25	TiNi	Ti_3Pt	−	51.3	33.3	15.4	74.8	0.5	24.7	−	−	−
A12	Ti25Ni45Pt30	$TiNi_3$	$Ti_2(Ni,Pt)_3$	−	25.2	45.8	29.0	39.1	32.6	28.3	−	−	−
A13	Ti40Ni30Pt30	TiNi	$Ti_2(Ni,Pt)_3$	−	48.8	16.8	34.4	40.4	30.7	28.9	−	−	−
A14	Ti10Ni55Pt35	$TiNi_3$	(Ni,Pt)	−	21.3	33.5	45.2	2.2	72.0	25.8	−	−	−
A15	Ti5Ni55Pt40	$TiNi_3$	(Ni,Pt)	−	21.7	27.9	50.4	0.9	62.3	36.8	−	−	−
A16	Ti50Ni10Pt40	TiNi	TiPt	−	50.6	13.5	35.9	50.3	5.4	44.3	−	−	−
A17	Ti55Ni5Pt40	TiNi	Ti_4Pt_3	−	51.2	14.6	34.2	58.3	2.1	39.6	−	−	−
A18	Ti32Pt68	Ti_3Pt_5	$TiPt_{3-}$	−	26.5	0.0	73.5	37.2	0.0	62.8	−	−	−

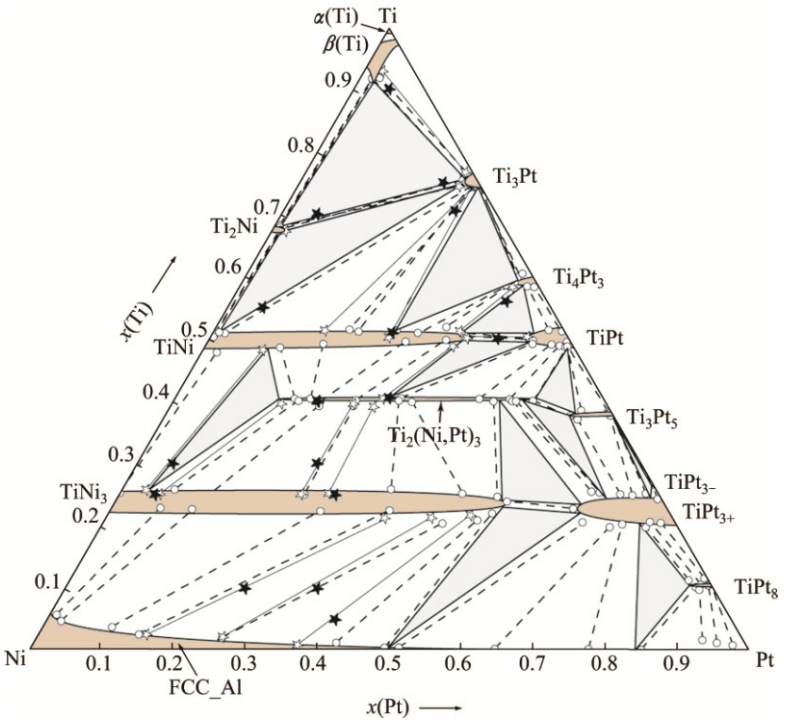

Fig. 5 Isothermal section of Ti−Ni−Pt ternary system at 1073 K (○—Phase equilibrium determined from diffusion couple; ☆—Phase equilibrium determined from equilibrated alloys; ★—Nominal composition of equilibrated alloys)

that Ti_3Pt_5 and $TiPt_{3-}$ are regarded as stable phases, and $TiPt_8$ is a stoichiometric binary phase. The ternary compound $Ti_2(Ni,Pt)_3$ was detected with composition of about 10.0%−45.2% Ni (molar fraction). Binary phases TiNi and $TiNi_3$ show remarkable ternary solubility, e.g., the solubility of Pt in TiNi and in $TiNi_3$ can be up to 35.9% and 54.4% (molar fraction), respectively.

3.2 Phase equilibria at 1173 K

BSE images obtained from the Ti−Ni−Pt diffusion triple after annealing at 1173 K for 500 h are shown in Fig. 6, where Ti_2Ni, TiNi and $TiNi_3$ were identifiable between blocks of Ti and Ni, and Ti_3Pt, Ti_4Pt_3, TiPt, Ti_3Pt_5, $TiPt_{3-}$, $TiPt_{3+}$ and $TiPt_8$ between Ti and Pt, respectively. And ternary phase $Ti_2(Ni,Pt)_3$ was also detected at 1173 K. The phase interfaces are illustrated in Fig. 7, and terminals of some typical tie-lines between two phases in equilibrium can be found in Table 4.

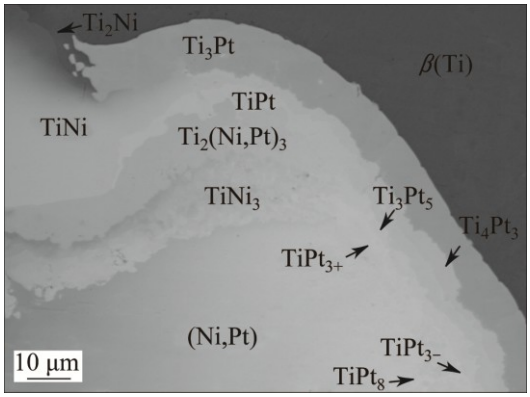

Fig. 6 Backscattered electron (BSE) image of Ti−Ni−Pt diffusion triple annealed at 1173 K for 500 h

To confirm or complete the phase relationship obtained through diffusion-triple, some alloys were synthesized and annealed at 1173 K and the microstructures of these alloys were further analyzed. As shown in Fig. 8(a), alloy B10 contains TiNi and Ti_3Pt, while two-phase microstructure $TiNi_3$ + (Ni,Pt) occurs in the alloy B14 (Fig. 8(b)). BSE image of alloy B15 presented in Fig. 8(c) shows two phases, the gray TiNi and the bright TiPt, in agreement with XRD results (Fig. 8(d)).

Constituent phases in these annealed alloys are summarized in Table 5. It is seen that phase equilibria measured through alloy sampling agree well with those through diffusion triples. Based on the measurements, isothermal section of the Ti−Ni−Pt ternary system at 1173 K is constructed, as demonstrated in Fig. 9, which consists of 12 three-phase regions. It is worth noting that two three-phase regions $Ti_2(Ni,Pt)_3$ + Ti_3Pt_5 + TiPt and $TiNi_3$ + $Ti_2(Ni,Pt)_3$ + $TiPt_{3+}$ at 1073 K change into another two three-phase regions $TiNi_3$ + $Ti_2(Ni,Pt)_3$ + Ti_3Pt_5 and $TiNi_3$ + Ti_3Pt_5 + $TiPt_{3+}$ at 1173 K. And similar to 1073 K, Ti_3Pt_5 and $TiPt_{3-}$ are also stable at 1173 K. The ternary phase $Ti_2(Ni,Pt)_3$ has a composition of 6.7%−47.1% Ni (molar fraction), showing little difference from that at 1073 K. In addition, ternary solubility in some binary compounds was remarkable, e.g., solubility of Pt in TiNi and in $TiNi_3$ can be up to 39.7% and 58.5% (molar fraction) at 1173 K, respectively.

3.3 Comparison of phase relations at 1073 and 1173 K

A preliminary comparison of phase relations at 1073 and 1173 K is carried out here. As can be seen in Figs. 5 and 9, some differences are manifested. Firstly, due to the polymorphic transformation of α(Ti)→β(Ti), i.e., α(Ti) is stable at 1073 K but transforms into β(Ti) at 1173 K, the two-phase region α(Ti)+β(Ti) at 1073 K disappears at 1173 K.

Secondly, the adjacent three-phase regions $TiNi_3$ + $Ti_2(Ni,Pt)_3$ + Ti_3Pt_5 and $TiNi_3$ + Ti_3Pt_5 + $TiPt_{3+}$ at 1173 K change into another two three-phase regions $Ti_2(Ni,Pt)_3$ + Ti_3Pt_5 + $TiPt_{3+}$ and $TiNi_3$ + $Ti_2(Ni,Pt)_3$ + $TiPt_{3+}$ at 1073 K. This implies that a typical peri-eutectoid reaction $TiNi_3$ + Ti_3Pt_5 → $Ti_2(Ni,Pt)_3$ + $TiPt_{3+}$ occurs at a certain temperature between 1073 and 1173 K.

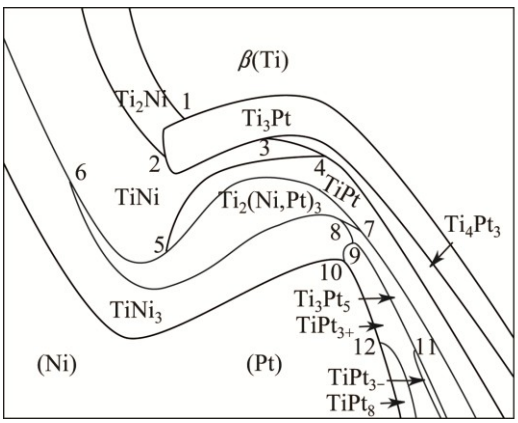

Ternary equilibria:
1: β(Ti)+Ti_2Ni+Ti_3Pt
2: Ti_2Ni+TiNi+Ti_3Pt
3: TiNi+Ti_3Pt+Ti_4Pt_3
4: TiNi+Ti_4Pt_3+TiPt
5: TiNi+TiPt+$Ti_2(Ni,Pt)_3$
6: TiNi+$TiNi_3$+$Ti_2(Ni,Pt)_3$
7: $Ti_2(Ni,Pt)_3$+Ti_3Pt_5+TiPt
8: $TiNi_3$+$Ti_2(Ni,Pt)_3$+Ti_3Pt_5
9: $TiNi_3$+Ti_3Pt_5+$TiPt_{3+}$
10: $TiNi_3$+$TiPt_{3+}$+(Ni,Pt)
11: Ti_3Pt_5+$TiPt_{3-}$+$TiPt_{3+}$
12: (Ni,Pt)+$TiPt_{3+}$+$TiPt_8$

Fig. 7 Schematic diagram of phase distribution of 1173 K diffusion triple (numbered tri-junction points (1−12) represent ternary equilibria existing in Ti−Ni−Pt system)

Table 4 Tie-lines determined through Ti−Ni−Pt diffusion triple treated at 1173 K

Tie-line	Phase composition (molar fraction)/%					
Phase 1/Phase 2	Phase 1			Phase 2		
	Ti	Ni	Pt	Ti	Ni	Pt
β(Ti)/Ti_2Ni	90.8	6.5	2.7	68.9	29.7	1.4
	90.6	6.8	2.6	69.0	28.9	2.1
β(Ti)/Ti_3Pt	91.2	6.2	2.6	75.6	1.4	23.0
	90.8	6.7	2.5	75.7	2.0	22.3
	91.2	6.3	2.5	75.7	1.6	22.7
Ti_2Ni/Ti_3Pt	69.0	28.9	2.1	75.6	1.0	23.4
	68.0	29.9	2.1	75.8	1.4	22.8
Ti_2Ni/TiNi	68.0	30.8	1.2	51.9	47.5	0.6
	67.9	30.0	2.1	52.3	46.1	1.6
TiNi/Ti_3Pt	51.3	15.3	33.4	73.5	0.4	26.1
	51.4	18.4	30.2	73.9	1.5	24.6
	51.2	27.5	21.3	74.9	0.8	24.3
	51.3	38.9	9.8	75.0	1.1	23.9
TiNi/Ti_4Pt_3	51.3	15.3	33.4	58.4	2.8	38.8
	51.3	10.3	38.4	57.8	2.7	39.5
Ti_3Pt/Ti_4Pt_3	75.1	0.5	24.4	58.5	1.5	40.0
	73.5	0.4	26.1	58.4	2.8	38.8
TiNi/TiPt	50.4	9.9	39.7	49.4	5.2	45.4
	50.3	10.4	39.3	50.4	4.8	44.8
Ti_4Pt_3/TiPt	58.4	0.8	40.8	50.4	0.4	49.2
	57.9	1.0	41.1	50.9	1.0	48.1
	58.3	2.6	39.1	50.5	4.4	45.1
TiNi/Ti_2(Ni,Pt)$_3$	48.1	15.5	36.4	41.3	30.5	28.2
	48.2	35.3	16.5	40.1	38.2	21.7
	48.6	38.8	12.6	40.5	40.8	18.7
	48.4	20.1	31.5	40.6	33.9	25.5
TiPt/Ti_2(Ni,Pt)$_3$	49.7	5.1	45.2	40.2	24.9	34.9
	48.8	2.0	49.2	40.8	8.6	50.6
	49.5	1.9	48.6	40.7	14.5	44.8
	50.0	2.5	47.5	40.8	19.1	40.1
	48.7	0.8	50.5	40.3	6.7	53.0
TiNi/$TiNi_3$	47.8	48.7	3.5	26.2	73.7	0.1
$TiNi_3$/Ti_2(Ni,Pt)$_3$	25.5	55.4	19.1	40.8	31.8	27.4
	26.0	65.5	8.5	40.9	39.7	19.4
	26.1	61.1	12.8	39.9	36.3	23.8
	25.6	33.8	40.6	40.3	14.9	44.8
	26.5	24.7	48.8	40.7	12.9	46.4
	25.2	18.3	56.5	40.5	11.1	48.4
TiPt/Ti_3Pt_5	48.5	0.1	51.4	37.7	1.8	60.5
Ti_3Pt_5/Ti_2(Ni,Pt)$_3$	37.9	2.1	60.0	40.0	6.5	53.5
	37.1	4.6	58.3	39.8	7.7	52.5
	37.5	5.4	57.1	40.7	10.2	49.1
$TiNi_3$/Ti_3Pt_5	25.2	17.3	57.5	37.3	5.2	57.5
Ti_3Pt_5/$TiPt_{3-}$	37.8	0.5	61.7	26.5	0.2	73.3
$TiPt_{3-}$/$TiPt_{3+}$	26.8	0.2	73.0	24.7	0.6	74.7
Ti_3Pt_5/$TiPt_{3+}$	36.9	1.5	61.6	24.8	3.1	72.1
	37.4	2.6	60.0	24.5	5.8	69.7
	37.5	4.1	58.4	24.7	8.8	66.5
$TiNi_3$/$TiPt_{3+}$	23.3	18.2	58.5	21.5	11.2	67.3
$TiNi_3$/(Ni,Pt)	21.4	39.7	38.9	3.7	73.4	22.9
	23.2	58.5	18.3	6.6	89.4	4.0
	23.0	46.0	31.0	4.3	81.9	13.8
	21.9	31.6	46.5	0.6	54.2	45.2
	23.6	28.5	47.9	0.3	45.1	54.6
	23.3	17.3	59.4	0.6	37.8	61.6
$TiPt_{3+}$/(Ni,Pt)	20.6	8.2	71.2	0.3	26.7	73.0
	20.5	1.2	78.3	0.1	5.9	94.0
	20.4	4.3	75.3	0.5	17.8	81.7
	21.0	10.2	68.8	0.5	34.3	65.2
$TiPt_{3+}$/$TiPt_8$	20.7	0.5	78.8	11.1	0.3	88.6
$TiPt_8$/(Ni,Pt)	10.1	0.7	89.2	0.5	1.1	98.4
	10.1	1.0	88.9	0.1	3.2	96.7

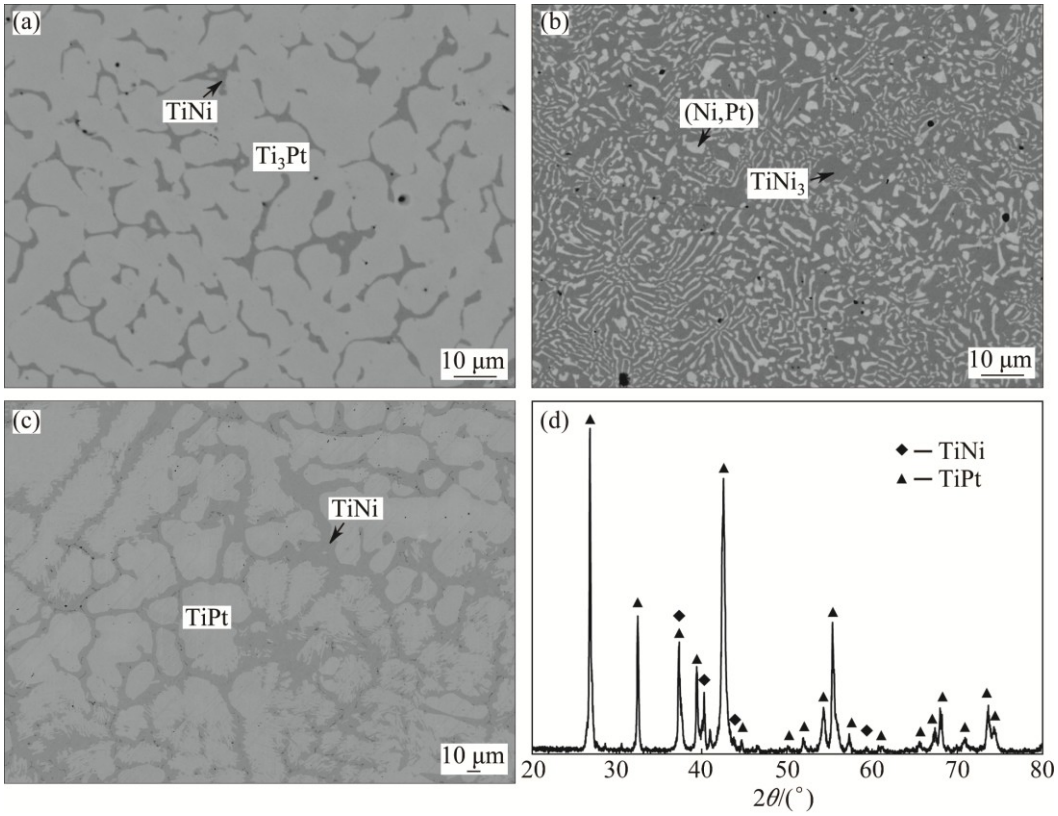

Fig. 8 BSE images of alloys annealed at 1173 K for 1000 h: (a) Alloy B10; (b) Alloy B14; (c) Alloy B15; (d) XRD pattern of alloy B15

Table 5 Phases and their compositions in Ti−Ni−Pt alloys annealed at 1173 K

Alloy	Composition (molar fraction)/%	Phase equilibrium			Phase composition (molar fraction)/%								
		Phase 1	Phase 2	Phase 3	Phase 1			Phase 2			Phase 3		
					Ti	Ni	Pt	Ti	Ni	Pt	Ti	Ni	Pt
B1	Ti25Ni70Pt5	$TiNi_3$	$Ti_2(Ni,Pt)_3$	−	25.7	68.1	6.2	38.8	45.1	16.1	−	−	−
B2	Ti30Ni65Pt5	TiNi	$TiNi_3$	−	47.0	43.2	9.8	25.1	71.2	3.7	−	−	−
B3	Ti55Ni40Pt5	Ti_2Ni	TiNi	Ti_3Pt	68.1	28.9	3.0	52.1	43.8	4.1	75.2	0.8	24.0
B4	Ti70Ni25Pt5	Ti_2Ni	Ti_3Pt	−	68.2	29	2.8	75.5	0.4	24.1	−	−	−
B5	Ti90Ni5Pt5	β(Ti)	Ti_3Pt	−	92.2	5.0	2.8	76.8	0.3	22.9	−	−	−
B6	Ti75Ni5Pt20	β(Ti)	Ti_2Ni	Ti_3Pt	97.4	0.2	2.4	68.8	28.9	2.3	77.3	1.0	21.7
B7	Ti10Ni65Pt25	$TiNi_3$	(Ni,Pt)	−	20.2	44.2	35.6	4.2	78.3	17.5	−	−	−
B8	Ti30Ni45Pt25	$TiNi_3$	$Ti_2(Ni,Pt)_3$	−	25.5	54.1	20.4	39.0	28.1	32.9	−	−	−
B9	Ti50Ni25Pt25	TiNi	Ti_3Pt	−	49.1	26.3	24.6	74.8	1.1	24.1	−	−	−
B10	Ti70Ni5Pt25	TiNi	Ti_3Pt	−	51.8	32.1	16.1	75.4	0.5	24.1	−	−	−
B11	Ti25Ni45Pt30	$TiNi_3$	$Ti_2(Ni,Pt)_3$	−	25.4	47.1	27.5	39.6	20.1	40.3	−	−	−
B12	Ti40Ni30Pt30	TiNi	$Ti_2(Ni,Pt)_3$	−	48.4	15.1	36.5	40.1	30.5	29.4	−	−	−
B13	Ti10Ni55Pt35	$TiNi_3$	(Ni,Pt)	−	20.1	38.8	41.1	1.4	69.2	29.4	−	−	−
B14	Ti5Ni55Pt40	$TiNi_3$	(Ni,Pt)	−	20.6	36.2	43.2	1.8	57.8	40.4	−	−	−
B15	Ti50Ni10Pt40	TiNi	TiPt	−	50.9	9.7	39.4	50.4	4.8	44.8	−	−	−
B16	Ti32Pt68	Ti_3Pt_5	$TiPt_{3-}$	−	26.7	0.0	73.3	37.3	0.0	62.7	−	−	−

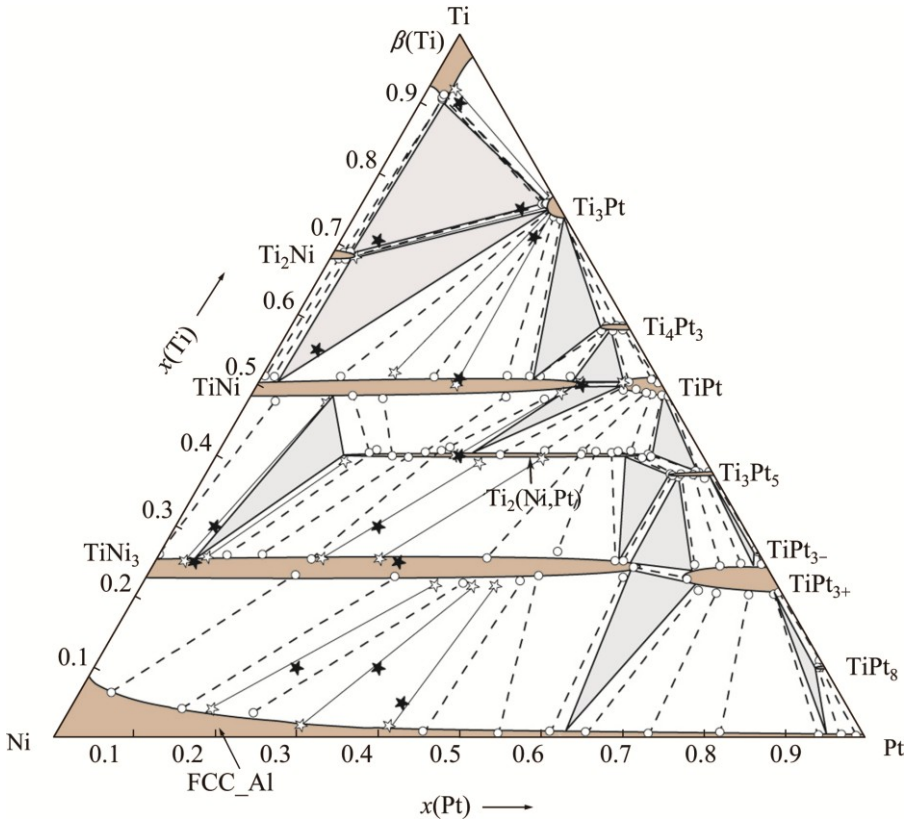

Fig. 9 Isothermal section of Ti−Ni−Pt ternary system at 1173 K (○—Phase equilibrium determined from diffusion couple; ☆—Phase equilibrium determined from equilibrated alloys; ★—Nominal composition of equilibrated alloys)

4 Conclusions

1) Isothermal sections of the Ti−Ni−Pt ternary system at 1073 and 1173 K have been measured in the present work, and an invariant transition reaction $TiNi_3 + Ti_3Pt_5 \rightarrow Ti_2(Ni, Pt)_3 + TiPt_{3+}$ at a temperature between 1073 and 1173 K was deduced.

2) Existence of the ternary phase $Ti_2(Ni, Pt)_3$ was confirmed, and its composition ranges from 10.0% to 45.2%Ni (molar fraction) at 1073 K and from 6.7% to 47.1%Ni (molar fraction) at 1173 K.

3) Binary phase Ti_3Pt_5 and $TiPt_{3-}$ were found to be stable at both 1073 and 1173 K, and $TiPt_8$ was determined to be a stoichiometric phase. In addition, remarkable ternary solubility of Pt in TiNi and $TiNi_3$ was detected.

References

[1] OTSUKA K, WAYMAN C M. Shape memory materials [M]. London: Cambridge University Press, 1999.

[2] SOEJIMA Y, MOTOMURA S, MITSUHARA M, INAMURA T, NISHIDA M. In situ scanning electron microscopy study of the thermoelastic martensitic transformation in Ti−Ni shape memory alloy [J]. Acta Materialia, 2016, 103: 352−360.

[3] SONG J, WANG L M, ZHANG X N, SUN X G, JIANG H, FAN Z G, XIE C Y, WU M H. Effects of second phases on mechanical properties and martensitic transformations of ECAPed TiNi and Ti−Mo based shape memory alloys [J]. Transactions of Nonferrous Metals Society of China, 2012, 22: 1839−1848.

[4] YAMABE-MITARAI Y, AROCKIAKUMAR R, WADOOD A, SURESH K S, KITASHIMA T, HARA T, SHIMOJO M, TASAKI W, TAKAHASHI M, TAKAHASHI S, HOSODA H. Ti(Pt,Pd,Au) based high temperature shape memory alloys [J]. Materials Today: Proceedings, 2015, 2: 517−522.

[5] MOSCA H O, BOZZOLO G, GROSSO M F. Atomistic modeling of ternary additions to NiTi and quaternary additions to Ni−Ti−Pd, Ni−Ti−Pt and Ni−Ti−Hf shape memory alloys [J]. Physica B, 2012, 407: 3244−3247.

[6] FRENZEL J, WIECZOREK A, OPAHLE I, MAAβ B, DRAUTZ R, EGGELER G. On the effect of alloy composition on martensite start temperatures and latent heats in Ni−Ti-based shape memory alloys [J]. Acta Materialia, 2015, 90: 213−231.

[7] MA J, KARAMAN I, NOEBE R D. High temperature shape memory alloys [J]. International Materials Reviews, 2010, 55: 257−315.

[8] SMIALEK J L, HUMPHYREY D L, NOEBE R D. Comparative oxidation kinetics of a NiPtTi high temperature shape memory alloy [J]. Oxidation of Metals, 2010, 74: 125−144.

[9] GONG C W, WANG Y N, YANG D Z, LIU X P. *R*-phase transformation of aged Ti−Ni shape memory alloy [J]. Transactions of Nonferrous Metals Society of China, 2005, 15: 1237−1241.

[10] GAO Y, ZHOU N, YANG F, CUI Y, KOVARIK L, HATCHER N. P-phase precipitation and its effect on martensitic transformation in (Ni,Pt)Ti shape memory alloys [J]. Acta Materialia, 2012, 60: 1514−1527.

[11] RIOS O, NOEBE R D, BILES T, GARG A, PALCZER A, SCHEIMAN D, SEIFERT H J, KAUFMAN M. Smart structures and materials: Active materials: Behavior and mechanics [M].

Bellingham, WA: SPIE, 2005: 376.
[12] YANG F, NOEBE R D, MILLS M J. Precipitates in a near-equiatomic (Ni+Pt)-rich TiNiPt alloy [J]. Scripta Materialia, 2013, 69: 713−715.
[13] NASH P, SINGLETON M F. The Ni−Pt (nickel−platinum) system [J]. Bull Alloy Phase Diagram, 1989, 10: 258−262.
[14] LU X G, SUNDMAN B, ÅGREN J. Thermodynamic assessments of the Ni−Pt and Al−Ni−Pt systems [J]. CALPHAD, 2009, 33: 450−456.
[15] KAUFMAN L, NESOR H. Coupled phase diagrams and thermochemical data for transition metal binary systems [J]. CALPHAD, 1978, 2: 81−108.
[16] MURRAY J L. Phase diagrams of binary titanium alloys [M]. Materials Park, OH: ASM International, 1987: 197−211.
[17] LIANG H, JIN Z P. A reassessment of the Ti−Ni system [J]. CALPHAD, 1993, 17: 415−426.
[18] SAUNDERS N. Ni-database [M]. Guildford: Thermo Tech Ltd., 1995.
[19] BELLEN P, KUMAR K C H, WOLLANTS P. Thermodynamic assessment of the Ni−Ti diagram [J]. Zeitschrift für Metallkunde, 1996, 87: 972−978.
[20] TANG W, SUNDMAN B, SANDSTRÖM R, QIU C. New modelling of the *B*2 phase and its associated martensitic transformation in the Ti−Ni system [J]. Acta Materialia, 1999, 47: 3457−3468.
[21] TOKUNAGA T, HASHIMA K, OHTANI H, HASEBE M. Thermodynamic analysis of the Ni−Si−Ti system using thermochemical properties determined from Ab Initio calculations [J]. Materials Transactions, 2004, 45: 1507−1514.
[22] KEYZER J D, CACCIAMANI G, DUPIN N, WOLLANTS P. Thermodynamic modeling and optimization of the Fe−Ni−Ti system [J]. CALPHAD, 2009, 33: 109−123.
[23] POVODEN-KARADENIZ E, CIRSTEA D C, LANG P, WOJCIK T, KOZESCHNIK E. Thermodynamics of Ti−Ni shape memory alloys [J]. CALPHAD, 2013, 41: 128−139.
[24] NISHIMURA H, HIRAMATSU T. On the corrosion resistance of titanium alloys: The equilibrium diagram of the titanium−platinum system [J]. Nippon Kinzoku Gakkaishi, 1957, 21: 469−473.
[25] MURRAY J L. The Pt−Ti (platinum−titanium) system [J]. Bull Alloy Phase Diagram, 1982, 3: 329−335.
[26] BIGGS T, CORNISH L A, WITCOMB M A, CORTIE M B. Revised phase diagram for the Pt−Ti system from 30 to 60 at.% platinum [J]. Journal of Alloys and Compounds, 2004, 375: 120−127.
[27] LI M, HAN W, C, LI C R. Thermodynamic assessment of the Pt−Ti system [J]. Journal of Alloys and Compounds, 2008, 461: 189−194.
[28] TRETYACHENKO L. MSIT ternary evaluation program [M]. Stuttgart: MSI, 2003: 54.
[29] VILLARS P, CALVERT L D. Pearson's handbook of crystallographic data for intermetallic phases [M]. USA: ASM International, Materials Park, 1991.
[30] HARRIS I R, NORMAN M, BRYANT A W. A study of some palladium-indium, platinum−indium and platinum−tin alloys [J]. Journal of the Less Common Metals, 1968, 16: 427−440.
[31] MASSALSKI T B, OKAMOTO H, SUBRAMANIAN P R, KACPRCZAK L. Binary alloy phase diagrams [M]. Materials Park, Ohio: ASM, 1990.
[32] VANREUTH E C, WATERSTRAT R M. Atomic ordering in binary *A*l5-type phases [J]. Acta Crystallographica Section B, 1968, 24: 186−196.
[33] DONKERSLOOT H C, van VUCHT J H N. Martensitic transformations in gold−titanium, palladium−titanium and platinum−titanium alloys near the equiatomic composition [J]. Journal of the Less Common Metals, 1970, 20: 83−91.
[34] SCHUBERT K, RAMAN A, ROSSTEUTSCHER W. Structural data of some metallic phases [J]. Naturwissenschaften, 1964, 51: 506−507.
[35] KRAUTWASSER P, BHAN S, SCHUBERT K. Structural investigations in systems Ti−Pd and Ti−Pt [J]. Zeitschrift für Metallkunde, 1968, 59: 724−729.
[36] SINHA A K. Close-packed ordered AB 3 structures in binary transition metal alloys [J]. Transactions of the Metallurgical Society of AIME, 1969, 245: 237−240.
[37] JEON M K, MCGINN P J. Effect of Ti addition to Pt/C catalyst on methanol electro-oxidation and oxygen electro-reduction reactions [J]. Journal of Power Sources, 2010, 195: 2664−2668.
[38] PIETROKOWSKY P. Novel ordered phase, Pt_8Ti [J]. Nature, 1965, 206: 291.
[39] HARA T, OHBA T, OTSUKA K, NISHIDA M. Phase transformation and crystal structures of Ti_2Ni_3 precipitates in TiNi [J]. Materials Transactions, 1997, 38: 277−284.
[40] JIN Z P. A study of the range of stability of sigma phase in some ternary systems [J]. Scandinavian Journal of Metallurgy, 1981, 10: 279−287.
[41] LIU H S, WANG Y M, ZHANG L G, CHEN Q, ZHENG F, JIN Z P. Determination of phase relations in the Co−Cu−Ti system by the diffusion triple technique [J]. Journal of Materials Research, 2006, 21: 2493−2503.

Ti−Ni−Pt 三元系相平衡关系

钟 跃，孙 悦，刘华山，蔡格梅，金展鹏

中南大学 材料科学与工程学院，长沙 410083

摘 要：采用扩散偶辅以平衡合金法的方法，利用电子探针 (EPMA) 和 X 射线衍射 (XRD) 等分析手段对 Ti−Ni−Pt 三元系的 1073 和 1173 K 等温截面的相关系进行实验测定。结果表明，三元化合物 $Ti_2(Ni, Pt)_3$ 和二元化合物 Ti_3Pt_5、$TiPt_3$ 在 1073 和 1173 K 是稳定的。部分二元化合物具有较大的第三组元固溶度，如在 1073 和 1173 K 下，Pt 在 TiNi 中的固溶度分别约为 36%和 40%(摩尔分数)。此外，在 1073~1173 K 的温度区间内存在零变量反应 $TiNi_3+Ti_3Pt_5\rightarrow Ti_2(Ni, Pt)_3+TiPt_3$。

关键词：Ti−Ni−Pt 三元系；相平衡；扩散偶；固溶度

(Edited by Bing YANG)